

LETTER TO THE EDITOR

Simultaneous optical and X-ray observations of a giant flare on the ultracool dwarf LP 412-31

B. Stelzer¹, J. H. M. M. Schmitt², G. Micela¹, and C. Liefke²

¹ INAF - Osservatorio Astronomico di Palermo, Piazza del Parlamento 1, 90134 Palermo, Italy
e-mail: stelzer@astropa.unipa.it

² Hamburger Sternwarte, Gojenbergsweg 112, 21029 Hamburg, Germany

Received 27 September 2006 / Accepted 18 October 2006

ABSTRACT

Cool stars are known to produce flares probably as a result of the magnetic reconnection in their outer atmospheres. We present simultaneous *XMM-Newton* optical *V* band and X-ray observations of the M8 dwarf LP412-31. During the observation a giant flare occurred, with an optical amplitude of 6 mag and total energy of 3×10^{32} erg in both the *V* band and soft X-rays. Both flare onset and flare decay were completely covered in both wavebands with a temporal resolution of 20 s, allowing determination of the flare time scales, as well as a study of the temperature evolution of the flaring plasma. The data are consistent with an impulsive energy release followed by radiative cooling without any further energy release during the decay phase. Our analysis suggests that the optical flare originates from a small fraction of the surface of LP 412-31, while the characteristic scale size of the flaring X-ray plasma is of the order of the stellar radius or larger. The absence of any small-scale variability in the light curve suggests a non-standard flare number energy distribution.

Key words. X-rays: stars – stars: activity – stars: flare – stars: low-mass, brown dwarfs – stars: coronae – stars: individual: LP 412-31

1. Introduction

Flares, i.e., short-term enhancements of the emission in various wavebands, belong to the most obvious manifestations of solar and stellar magnetic activity. During a solar white-light flare, the footpoints of magnetic loops light up in the optical and ultraviolet emission lines and the continuum. Intense X-ray emission goes along with such events and is ascribed to the filling of these loops with heated plasma evaporated off the chromospheric layers along the magnetic field lines into the corona (the “chromospheric evaporation scenario”, e.g., Antonucci et al. 1984). Depending on the flare frequency distribution, quiescent high-energy emission might be due to a super-position of unresolved micro-flares (Krucker & Benz 1998; Aschwanden et al. 2000).

On dM(e) stars (“flare stars”) flares are far more frequently observed (mostly in *U* band or $H\alpha$) than on the Sun. However, because of significant logistic and observational difficulties, simultaneous data taken in different wavebands, indispensable for testing the validity of the above scenario, has rarely been secured. The situation becomes even worse for the low-mass end of the main sequence. The fraction of $H\alpha$ emitters among the M dwarf population decreases quickly for ultracool dwarfs beyond spectral type $\approx M7$, yet objects of late-M or L spectral type can produce spectacular $H\alpha$ flares (Liebert et al. 1999, 2003; Fuhrmeister & Schmitt 2004). X-ray emission has been observed only from a rather small number of ultracool dwarfs, and in most of these cases X-ray detections were made only during flares (Fleming et al. 2000; Rutledge et al. 2000; Schmitt & Liefke 2002; Stelzer 2004). None of these observations was accompanied by concurrent observations in other wavebands. Optical broad-band observations of (ultracool) dwarfs are more abundant. However, most of the available data do not have the temporal resolution required to follow the rapid evolution of the

photospheric and chromospheric emission. The observed magnitude increases in the optical wavebands can be enormous. Some – rare – examples of huge optical events on M dwarfs with amplitudes >6 mag in optical and UV bands, respectively, are presented by Pagano et al. (1997) and Rokenfeller et al. (2006). Observational records of nine superflares in various wavebands were collected by Schaefer et al. (2000), but these observations lack any information on time evolution.

In this letter we present a giant X-ray flare on the M8 dwarf LP 412-31, recorded with the *XMM-Newton* satellite with a time resolution of a few seconds simultaneously in soft X-rays and in the *V* band. LP 412-31 was originally identified in the proper motion survey of Luyten (1979) and first classified as a very late M dwarf by Kirkpatrick et al. (1995). Since then it has frequently been used as a reference star for spectral type M8, although little is actually known about its stellar parameters. LP 412-31 is located at a distance of 14.6 ± 0.1 pc (Reid & Cruz 2002). Mohanty & Basri (2003) derive an effective temperature of 2550 K, and we obtain $L_{\text{bol}} = 2.09 \times 10^{30}$ erg s⁻¹ from the *J* band magnitude using the bolometric correction $(BC)_J = 1.95$ (Reid et al. 2001). According to the evolutionary models of Chabrier et al. (2000), LP 412-31 is close to the bottom of the main sequence ($0.04\text{--}0.1 M_{\odot}$) and is moderately young (≈ 0.3 Gyr). LP 412-31 belongs to the strongest $H\alpha$ emitters of its spectral type. Its $H\alpha$ equivalent width has been measured at various epochs with values between 20–80 Å (Martín et al. 1996; Gizis et al. 2000; Reid et al. 2002; Mohanty & Basri 2003). The magnetic field strength of LP 412-31 (>3.9 kG) is among the highest in the sample of ultracool dwarfs studied by Reiners & Basri (2006). No reports of X-ray emission from LP 412-31 exist in the literature, and in particular the *ROSAT* All-Sky Survey data implies a flux limit of $<2 \times 10^{-13}$ erg cm⁻² s⁻¹, corresponding to a soft X-ray luminosity of $<5 \times 10^{27}$ erg s⁻¹.

2. Observations and data analysis

We observed LP 412-31 for 40 ks with *XMM-Newton*¹ (ObsID 0300170101) and analysed the data with the *XMM-Newton* Science Analysis system (SAS) version 6.5.0.

The thin filter was inserted for all three European Photon Imaging Camera (EPIC) instruments. In this paper we use only data from the EPIC/pn CCD. Data processing included standard filtering of the event list. After removing time intervals of high background using a screening algorithm, the EPIC/pn yielded 25 ks of useful science data. Visual inspection of the X-ray image showed an unexpectedly bright X-ray source coincident with LP 412-31. For the temporal and spectral analysis of this source we used the source photons extracted from a 30'' circle centred on the X-ray position of LP 412-31 and background photons from a circle of equal size positioned on a source-free adjacent position.

The Optical Monitor (OM) onboard *XMM-Newton* was operated in the standard IMAGE FAST Mode with the V band filter. For this work we use only data from the central fast-mode window of 10.5'' × 10.5'' pixels read out with a time resolution of 20 s. For technical reasons the OM observation had to be divided into nine exposures (7 × 4400 s, 1 × 3700 s, and 1 × 2960 s) separated by an overhead of ~0.3 ks. Thus, there is almost complete time coverage of the X-ray observation in the V band with high time resolution. The OM data from the central fast-mode window was processed with standard SAS procedures, resulting in a sequence of V band count rates with a time resolution of 20 s. For the conversion of OM count rates into magnitudes and fluxes, we used the numbers given in the *XMM-Newton* SAS Users' Guide².

An inspection of the lightcurves of both the X-ray and optical data showed the presence of a huge flare at about one third into the observation, but a weak signal without any signs of variability during the rest of the observation. Substantial precursor activity before the actual flare onset is clearly visible in the X-ray data (EPIC/pn count rate enhanced by a factor ≈ 30 with respect to the pre- and post-flare quiescent emission). Figure 1 shows a fraction of the recorded lightcurves, starting with the X-ray flare precursor, during which no significant activity is seen in the OM data. In Table 1 we summarise count rates, magnitudes, and luminosities measured during the different observed activity states.

For the quiescent state before and after the flare (not shown in Fig. 1), we measured an X-ray luminosity of $\log L_{X,q} \sim 27.2 \text{ erg s}^{-1}$, corresponding to a fractional X-ray luminosity of $\log(L_{X,q}/L_{\text{bol}}) \sim -3.1$. This represents the first detection of (quiescent) X-ray emission for LP 412-31. Our measurement puts LP 412-31 at the upper end of the activity range for flare stars, which is not unexpected considering its strong and variable H α emission and strong magnetic field. The quiescent OM V band count rate translates into a V band magnitude of ~ 19 mag, in good agreement with the literature value (Dahn et al. 2002).

Both visual inspection of the lightcurves and Spearman's and Kendall's rank correlation tests are consistent with a time delay of ≤ 20 –40 s (1–2 bins) between the optical and X-ray bands. Both EPIC/pn and OM count rates increase by factors of 200–300 from quiescence to their peak luminosities of $4.6 \times 10^{29} \text{ erg s}^{-1}$ and $2.8 \times 10^{30} \text{ erg s}^{-1}$, respectively. Specifically,

¹ The satellite and its instruments are described in a Special Issue of *Astronomy & Astrophysics* Vol. 365 (Jan. 2001).

² http://xmm.vilspa.esa.es/external/xmm_user_support/documentation/uhb/index.html

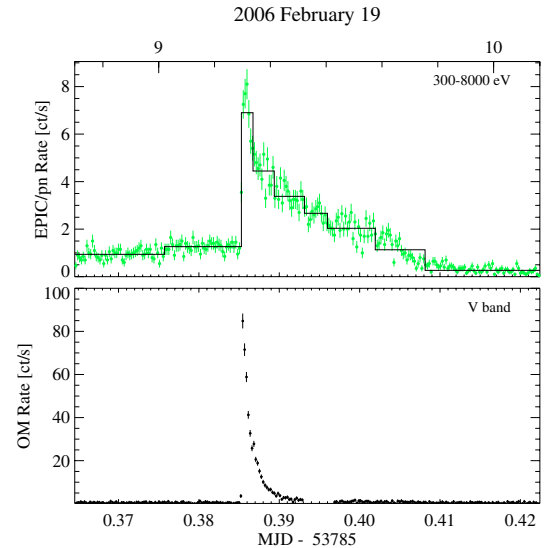


Fig. 1. Fraction of the *XMM-Newton* lightcurves of LP 412-31 showing the giant flare and the precursor state. Both EPIC/pn and OM data are binned to the 20 s time resolution given by the OM. The EPIC/pn lightcurve is overlaid by the blocks derived in the ML analysis. The last block is not seen because of the restricted x-scale.

the V magnitude rises within 40 s to a maximum of 13.1 mag ($\Delta V \approx 6$ mag), whence it decays exponentially back to quiescence on a decay time scale $\tau_{\text{OM}} \sim 90$ s. The decay of the X-ray light curve is far more prolonged. It is fast initially, but slows down soon after and can be roughly described by two exponentials, a first one with a decay time scale similar to the optical decay ($\tau_{1,\text{pn}} \sim 150$ s) and a second exponential that decays with $\tau_{2,\text{pn}} \sim 1000$ s.

We analysed the EPIC/pn light curve with a binning independent maximum likelihood (ML) method described in detail by Stelzer et al. (2006). We used this technique first to find possible background variations and then subtracted the background from the events listed at the source position, making use of the previously determined segmentation of the background signal. The result is a background-subtracted net source-photon events list, to which the ML algorithm is applied. In Fig. 1 the binned lightcurve is overlaid by the constant-rate blocks resulting from the ML analysis with an imposed minimum number of 500 cts per block and a confidence level for change points of 99.9%. Since the data before the flare precursor (not shown in Fig. 1) consists of fewer than 500 cts, we started the ML analysis with the flare precursor. This procedure results in a division of the lightcurve into ten intervals of constant signal that we used for spectral analysis.

For each of the ten blocks, as well as for the first 6 ks of the observation (representing the quiescent emission before the flare), a source and background spectrum, a response matrix, and an ancillary response file were extracted with standard *XMM-Newton* SAS tools. We first fitted the quiescent spectrum within the XSPEC v11.3 environment using a two-component APEC thermal spectrum with a photo-absorption term. The spectral fitting shows the absorbing column to be very low as expected for a nearby star. For the subsequent analysis of the flare spectra we froze all parameters of the quiescent model and added a spectral model describing the additional flare emission.

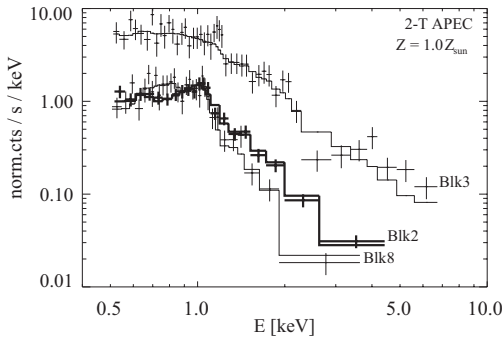
For the flare component, we tested a series of one-temperature (1-T) and two-temperature (2-T) thermal models with global abundance Z set to different values ($Z = 0.3 Z_{\odot}$,

Table 1. Count rates, magnitudes, and luminosities for LP412-31 in different activity states.

| | Pre-flare ^a | Flare peak | Post-flare ^b |
|------------------------------|--------------------------------|--------------------------------|--------------------------------|
| OM | | | |
| C [cts s ⁻¹] | 0.50 ± 0.20 | 84.83 ± 3.47 | 0.30 ± 0.08 |
| V [mag] | 18.7 ± 0.4 | 13.1 ± 0.1 | 19.3 ± 0.2 |
| L_V [erg s ⁻¹] | $(1.6 \pm 0.5) \times 10^{28}$ | $(2.8 \pm 0.1) \times 10^{30}$ | $(9.8 \pm 2.0) \times 10^{27}$ |
| EPIC/pn | | | |
| C [cts s ⁻¹] | 1.089 ± 0.067 | 8.100 ± 0.636 | 0.042 ± 0.003 |
| L_X [erg s ⁻¹] | $(6.1 \pm 0.4) \times 10^{28}$ | $(4.6 \pm 0.4) \times 10^{29}$ | $(1.6 \pm 0.2) \times 10^{27}$ |

^a Defined by ML blocks No. 1 and 2 representing the flare precursor activity (enhanced count rate in EPIC/pn with respect to quiescence; see text).

^b Defined by ML block No.10 comprising all data after the flare decay.

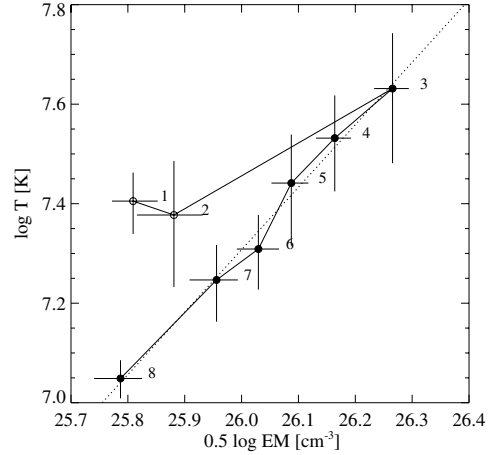

Fig. 2. EPIC/pn spectrum and best-fit model for the flare precursor (Blk 2; thick lines), flare peak (Blk 3), and the end of the flare decay (Blk 8).

$Z = 1.0 Z_{\odot}$, and Z a free-fit variable). The 1-T models turned out to be unacceptable for most time segments. The only approach that yields a statistically acceptable description and well-constrained parameters for all spectra is the 2-T model with $Z = 1.0 Z_{\odot}$, considered the best fit model (see Fig. 2 for a selection of spectra). A mean temperature T was computed for each spectrum from an emission measure (EM) weighted sum of both fit components. The total EM is given by the sum of the EM s of both components. The resulting T vs. \sqrt{EM} diagram is plotted in Fig. 3 and will be used as a diagnostic for the flare evolution.

3. Discussion and conclusions

3.1. Optical and X-ray properties of the giant flare

To derive quantitative information from the optical signal we chose a description of the flare photosphere in terms of blackbody emission with effective temperature as a free parameter. Although the flaring photosphere is likely not a perfect blackbody, at least in the V band there are no strong emission lines (de Jager et al. 1989), and blackbody models have provided a reasonable approximation for flare continua on earlier M dwarfs (Hawley & Fisher 1992). Using the V filter response curve, the luminosity derived from the OM count rate (see Table 1) can be corrected for the temperature-dependent out-of-band flux (“bolometric correction”). Assuming a photospheric “flare temperature” $T_{\text{eff}} = 9500$ K, we obtained an optical flare peak luminosity of $L_{\text{bol,peak}} = 4.7 \times 10^{30}$ erg s⁻¹; raising T_{eff} to 15 000 K increases this luminosity by a factor of two. With an assumed stellar radius of $0.12 R_{\odot}$, the area of the flaring region on the star is $(3.4\text{--}13) \times 10^{18}$ cm², i.e., the flare occupied <1% of the surface of LP412-31. This compares well with the flare area sizes


Fig. 3. Time evolution of the coronal temperature and emission measure. Open circles denote the flare precursor, filled circles the flare decay. The dotted line represents a linear least-square fit to the flare decay, which yields a slope $\zeta = 1.25$. Numbers in the plot refer to the constant rate blocks determined with the ML analysis.

determined for UV Cet (de Jager et al. 1989) and for solar white-light flares (Xu et al. 2006).

We determined the physical parameters of the X-ray emitting region making use of the hydrodynamic flare model and its calibration to the EPIC/pn spectral response described by Reale et al. (2004). This approach implies that we interpreted the flare on LP412-31 as a compact loop flare. From the measured slope of $\zeta = 1.25$ of the flare evolution in the $\log T - \log \sqrt{EM}$ plane (see Fig. 3) and the observed $\log T_{\text{peak}} [\text{K}] = 7.65$, we find a (half) loop length of $L \approx 1.4 \times 10^{10}$ cm, i.e., a value higher than the radius of LP412-31. Assuming that the cross section of the flaring loop is given by the size of the optical flaring region, we computed a volume of $V_{\text{flare}} \approx (0.9\text{--}3.6) \times 10^{29}$ cm³ and, using the observed peak EM of 3.4×10^{52} cm⁻³, a mean plasma density of $(3\text{--}6) \times 10^{11}$ cm⁻³. In principle, the expectation of high density could be checked with the *XMM-Newton* RGS data, but unfortunately, due to the high flare plasma temperature, the signal in the O VII triplet (which would be sensitive to densities in that range) is so weak that no quantitative conclusions can be drawn from that data. At any rate, the size of the flaring region in X-rays is quite large and of the order of the stellar dimensions. Therefore considerable heating of the non-flaring atmosphere as well must occur as a result of its illumination by the hot flaring plasma. Furthermore, the derived length scale L must be filled with plasma quite rapidly. Assuming ad hoc expansion velocities of 1000 km s⁻¹, the typical filling time scales are of the order of $50\text{--}100$ s, which is comparable to the possible observed delay between flare onset and flare maximum. Also, considerable line shifts and broadening are expected that, however, cannot be diagnosed because of the low signal-to-noise of the presently available data. Finally, we can estimate the total thermal energy content $E_{\text{th,X}} = 3nkTV$ of the X-ray plasma at flare peak. Using the above numbers, we find $E_{\text{th,X}} = (1\text{--}2) \times 10^{33}$ erg.

In terms of optical amplitude, this flare on LP412-31 is among the largest recorded in detail throughout the history of stellar flare observations, and it belongs to the very few flares allowing an assessment of the overall energy budget both in X-ray and optical light. The emitted flare energy amounts to 3×10^{32} erg, each in the V band and in soft X-rays, values clearly at the upper end of the range observed for field flare stars but lower than those for T Tauri stars (Fernández et al. 2004;

Stelzer et al. 2006). The total radiated energy is thus at least $E_{\text{rad}} \approx 6 \times 10^{32}$ erg, and this is obviously a lower limit, since energy may be radiated in other wavebands. We further find that the energy radiated in the soft X-ray band is roughly of the same order as the value derived for the thermal energy content of the coronal plasma at flare peak, and hence there appears to be no substantial energy release required in the flare decay phase. This is consistent with the fact that the observed value for the slope in the T vs. \sqrt{EM} diagram is close to the limiting value of $\zeta = 1.3$, above which the heating time scale is zero in the hydrodynamic model of Reale et al. (2004).

It is assumed in the standard flare scenario that the total energy released in the flare is ultimately derived from energy stored in the magnetic field and converted into other forms of energy during the flare. Comparing the magnetic energy density to the radiated flare energy and flare volume derived above, we can compute the mean magnetic field that must be annihilated in the corona in order to provide the observed energy. We find $B_{\text{annih}} \approx (140\text{--}280)\text{G}$. The minimal field necessary for confinement is the equipartition field, $B_{\text{eq}} \approx 310\text{--}430\text{G}$, and obviously this field must not be destroyed in the course of the flare progress. The total coronal magnetic field prior to flare onset must thus be in the range $450\text{--}710\text{G}$ in a volume of $V_{\text{flare}} \approx (9\text{--}36) \times 10^{28} \text{cm}^3$. If the annihilated field is limited to a smaller volume, the field strength must be even larger. The flare onset is quite rapid and the conversion of magnetic energy into thermal energy occurs within at most $20\text{--}40\text{s}$.

3.2. LP 412-31 in the context of stellar flares

So far the most detailed example of a coordinated optical and X-ray observation of a large flare on an M dwarf presented in the literature is an *XMM-Newton* observation of Proxima Cen (M5.5e) by Güdel et al. (2004). The peak X-ray luminosities of the flares on Proxima Cen and LP 412-31 are quite similar, and it is instructive to compare them in more detail. As in LP 412-31, the optical flare on Proxima Cen was shorter than the X-ray event, in line with the expectation from a flare scenario where the optical burst is considered as a proxy of the initial (impulsive) heating of chromospheric plasma by accelerated electrons. However, there are marked phenomenological differences between the two events. The Proxima Cen X-ray flare was a long-duration event with a rise time of 12 min and decay time of a significant fraction of a day, in contrast to the short flare observed on LP 412-31. The onset of the optical event preceded that of the X-ray flare in the case of Proxima Cen, while any time lags in LP 412-31 are below the time resolution of 20 s. In the chromospheric evaporation scenario, stellar flares are expected to peak in the optical before the X-rays, but observational evidence was found only in few cases due to the lack of simultaneous multi-band data (Schmitt et al. 1993; Mitra-Kraev et al. 2005).

The EPIC light curve of Proxima Cen displays – unlike the case of LP 412-31 – next to a major flare with a total energy $\approx 1.5 \times 10^{32}$ erg, several small events with energies of a few 10^{29} to $\approx 10^{31}$ erg. Such observations of lower-level flaring have led to the idea of stellar coronal nano-flare heating. Studies of solar flares and some bright flare stars suggest that the energy distribution of flares follows a power law with a slope ≈ -2 in its differential form (e.g., Aschwanden et al. 2000; Audard et al. 2000). A systematic analysis of X-ray flaring in a sample of pre-main sequence stars in the Taurus star forming region has yielded similar results (Stelzer et al. 2006). In the context of LP 412-31, the question arises whether the observed giant flare

can be interpreted as the “high energy tail” of a canonical flare frequency distribution. According to Stelzer et al. (2006) we expect to be sensitive to X-ray events with relative amplitude $A_{\text{rel}} = (R_{\text{max}} - R_{\text{Q}})/R_{\text{Q}} > 0.3$, where R_{max} and R_{Q} are the maximum and the quiescent soft X-ray count rate, given the sensitivity limit imposed by Poisson statistics and the observed quiescent EPIC/pn count rate of LP 412-31. This limit corresponds to flares with a peak luminosity of $\log L_{\text{X}} [\text{erg s}^{-1}] \sim 27.3$. Assuming a duration of 5000 s for such micro-flares – probably a conservative estimate considering the short duration of the observed giant flare – the emitted energy of such events would be 3×10^{30} erg. If the number distribution of flares on LP 412-31 were as observed for other stars, one would expect to see ≈ 100 such events for each giant flare, in clear contrast to our EPIC/pn data. Depending on the absolute flare frequency, it could in principle be possible to have failed to detect smaller flares because of the limited observing time; however, it is just as possible that the actual flare energy distribution of LP 412-31 is rather flat. In this case, the origin of the quiescent X-ray emission (often considered to be composed of unresolved micro- and nano-flares) remains unclear. Future multi-wavelength monitoring observations of ultracool dwarfs will prove useful for constraining the structure and energetics of their outer atmospheres.

Acknowledgements. We thank the referee C. Bailer-Jones for his quick response. BS and GM acknowledge funding by ASI-INAF contract I/023/05/0. CL was supported by DLR grant OR5010. This work is based on observations obtained with *XMM-Newton*, an ESA science mission with instruments and contributions directly funded by ESA Member States and NASA.

References

- Antonucci, E., Gabriel, A. H., & Dennis, B. R. 1984, *ApJ*, 287, 917
 Aschwanden, M. J., Tarbell, T. D., Nightingale, R. W., et al. 2000, *ApJ*, 535, 1047
 Audard, M., Güdel, M., Drake, J. J., & Kashyap, V. L. 2000, *ApJ*, 541, 396
 Chabrier, G., Baraffe, I., Allard, F., & Hauschildt, P. 2000, *ApJ*, 542, 464
 Dahn, C. C., Harris, H. C., Vrba, F. J., et al. 2002, *AJ*, 124, 1170
 de Jager, C., Heise, J., van Genderen, A. M., et al. 1989, *A&A*, 211, 157
 Fernández, M., Stelzer, B., Henden, A., et al. 2004, *A&A*, 427, 263
 Fleming, T. A., Giampapa, M. S., & Schmitt, J. H. M. M. 2000, *ApJ*, 533, 372
 Fuhrmeister, B., & Schmitt, J. H. M. M. 2004, *A&A*, 420, 1079
 Gizis, J. E., Monet, D. G., Reid, I. N., et al. 2000, *AJ*, 120, 1085
 Güdel, M., Audard, M., Reale, F., Skinner, S. L., & Linsky, J. L. 2004, *A&A*, 416, 713
 Hawley, S. L., & Fisher, G. H. 1992, *ApJS*, 78, 565
 Kirkpatrick, J. D., Henry, T. J., & Simons, D. A. 1995, *AJ*, 109, 797
 Krucker, S., & Benz, A. O. 1998, *ApJ*, 501, L213
 Liebert, J., Kirkpatrick, J. D., Reid, I. N., & Fisher, M. D. 1999, *ApJ*, 519, 345
 Liebert, J., Kirkpatrick, J. D., Cruz, K. L., et al. 2003, *AJ*, 125, 343
 Luyten, W. J. 1979, LHS Catalogue, University of Minnesota, Minneapolis
 Martín, E. L., Rebolo, R., & Zapatero-Osorio, M. R. 1996, *ApJ*, 469, 706
 Mitra-Kraev, U., Harra, L. K., Güdel, M., et al. 2005, *A&A*, 431, 679
 Mohanty, S., & Basri, G. 2003, *ApJ*, 583, 451
 Pagano, I., Ventura, R., Rodonò, M., Peres, G., & Micela, G. 1997, *A&A*, 318, 467
 Reale, F., Güdel, M., Peres, G., & Audard, M. 2004, *A&A*, 416, 733
 Reid, I. N., & Cruz, K. L. 2002, *AJ*, 123, 2806
 Reid, I. N., Burgasser, A. J., Cruz, K. L., Kirkpatrick, J. D., & Gizis, J. E. 2001, *AJ*, 121, 1710
 Reid, I. N., Kirkpatrick, J. D., Liebert, J., et al. 2002, *AJ*, 124, 519
 Reiners, A., & Basri, G. 2006, *ApJ*, in press
 Rockefeller, B., Bailer-Jones, C. A. L., Mundt, R., & Ibrahimov, M. A. 2006, *MNRAS*, 367, 407
 Rutledge, R. E., Basri, G., Martín, E. L., & Bildsten, L. 2000, *ApJ*, 538, L141
 Schaefer, B. E., King, J. R., & Deliyannis, C. P. 2000, *ApJ*, 529, 1026
 Schmitt, J. H. M. M., & Liefke, C. 2002, *A&A*, 382, L9
 Schmitt, J. H. M. M., Haisch, B., & Barwig, H. 1993, *ApJ*, 419, L81
 Stelzer, B. 2004, *ApJ*, 615, L153
 Stelzer, B., Flaccomio, E., Briggs, K., et al. 2006, *A&A*, in press
 Xu, Y., Cao, W., Liu, C., et al. 2006, *ApJ*, 641, 1210